2014

The Most Distant Stars in the Milky Way

John J. Bochanski
Haverford College, jbochans@haverford.edu

Beth Willman
Haverford College

Nelson Caldwell

Robyn Sanderson

Andrew A. West

The Astrophysical Journal Letters, 790:L5 (6pp), 2014 July 20 doi:10.1088/2041-8205/790/1/L5

THE MOST DISTANT STARS IN THE MILKY WAY

John J. Bochanski[1], Beth Willman[1], Nelson Caldwell[2], Robyn Sanderson[3], Andrew A. West[4], Jay Strader[5], and Warren Brown[2]
[1] Haverford College, 370 Lancaster Ave, Haverford, PA 19041, USA; jbochans@haverford.edu
[2] Harvard-Smithsonian Center for Astrophysics, Cambridge, MA 02138, USA
[3] Kapteyn Astronomical Institute, P.O. Box 800, 9700 AV Groningen, The Netherlands
[4] Department of Astronomy, Boston University, 725 Commonwealth Avenue, Boston, MA 02215, USA
[5] Michigan State Astronomy Group, Michigan State University, Biomedical Physical Sciences Building, 567 Wilson Road, Room 3261 East Lansing, MI 48824-2320, USA
Received 2014 May 6; accepted 2014 June 20; published 2014 July 3

ABSTRACT

We report on the discovery of the most distant Milky Way (MW) stars known to date: ULAS J001535.72+015549.6 and ULAS J074417.48+253233.0. These stars were selected as M giant candidates based on their infrared and optical colors and lack of proper motions. We spectroscopically confirmed them as outer halo giants using the MMT/Red Channel spectrograph. Both stars have large estimated distances, with ULAS J001535.72+015549.6 at 274 ± 74 kpc and ULAS J074417.48+253233.0 at 238 ± 64 kpc, making them the first MW stars discovered beyond 200 kpc. ULAS J001535.72+015549.6 and ULAS J074417.48+253233.0 are both moving away from the Galactic center at 52 ± 10 km s^{-1} and 24 ± 10 km s^{-1}, respectively. Using their distances and kinematics, we considered possible origins such as: tidal stripping from a dwarf galaxy, ejection from the MW's disk, or membership in an undetected dwarf galaxy. These M giants, along with two inner halo giants that were also confirmed during this campaign, are the first to map largely unexplored regions of our Galaxy's outer halo.

Key words: Galaxy: halo – Galaxy: stellar content – Galaxy: structure – stars: late-type

Online-only material: color figures

1. INTRODUCTION

The outer halo of our Milky Way (MW) has yet to be comprehensively mapped. Surveys such as the Sloan Digital Sky Survey (SDSS; York et al. 2000) have yielded large samples of metal-poor main sequence turnoff stars, which have been used to map out the MW's inner halo (e.g., Bell et al. 2008) to distances of $d \lesssim 50$ kpc over large areas of sky. Other stellar tracers, such as RR Lyrae (RRL) stars (e.g., Drake et al. 2013), red giant branch stars (e.g., Helmi et al. 2003; Xue et al. 2014) and blue horizontal branch (BHB) stars (e.g., Schlaufman et al. 2009), have also been used to map the Galactic halo to distances out to $d \sim 120$ kpc. However, very few stars at $d \gtrsim 120$ kpc have been identified mostly due to the faint limits of large surveys ($r \lesssim 21$). Table 1 lists the known stars at $d > 120$ kpc.

This severely incomplete picture of the Galaxy's outermost reaches limits our understanding of halo formation and evolution. Stars are not expected to be able to form *in situ* at outer halo distances (e.g., Zolotov et al. 2009). Instead, lone stars found at truly large distances ($d \gtrsim 200$ kpc) could mark the presence of outer halo substructure from accreted dwarf galaxies (e.g., Bullock & Johnston 2005; Majewski et al. 2003), or result from a star being ejected from the Galactic center or disk (e.g., Brown et al. 2005). If they are bound to the MW, distant halo stars could be used to measure the MW's virial mass, which is uncertain by a factor of ~3, ranging from ~0.7 to $2 \times 10^{12}\ M_{\odot}$ (Sofue 2012; Deason et al. 2012b; Burch & Cowsik 2013; Irrgang et al. 2013).

M giants currently offer the best opportunity to probe the MW's outer halo with existing surveys. They are intrinsically bright, with typical bolometric luminosities of $\log L/L_{\odot} \sim$ 3–4. Given their relatively cool effective temperatures, near infrared (NIR) surveys, such as the Two-Micron All Sky Survey (2MASS; Skrutskie et al. 2006) and the UKIRT Infrared Deep Sky Survey (UKIDSS; Lawrence et al. 2007), are especially sensitive to M giants. M giants in 2MASS were used to extensively map out the Sagittarius dwarf galaxy (Sgr; Majewski et al. 2003; Law & Majewski 2010). SDSS observations of M giants were also used to map out the Sgr tidal remnants, including the structure at distances near ~100 kpc (Yanny et al. 2009; Belokurov et al. 2014). The UKIDSS data, which has a faint limit 3–4 mag deeper than 2MASS, is sensitive to the most luminous M giants to distances beyond the MW's virial radius (~180–300 kpc; Klypin et al. 2002; Deason et al. 2012a; Piffl et al. 2014, and references therein).

In Bochanski et al. (2014, hereafter Paper I), we assembled a catalog of 404 M giant candidates, which were selected based on their NIR colors from the UKIDSS Large Area Survey (ULAS), optical colors from SDSS, and proper motions. In this Letter, we report on the discovery of two extremely distant M giants from this catalog, ULAS J001535.72+015549.6 and ULAS J074417.48+253233.0 (hereafter ULAS J0015+01 and ULAS J0744+25). These stars were spectroscopically confirmed as M giants, at distances of ~270 and 240 kpc (and at least 180 and 130 kpc, respectively, depending on metallicity). They are the first MW stars identified beyond 200 kpc, and potentially beyond the virial radius. We present our observations in Section 2. Our spectral type determinations, distance estimates and radial velocity measurements are described in Section 3. In Section 4 we discuss our hypotheses for the origins of these stars.

2. OBSERVATIONS

The details of our M giant candidate selection are contained in Paper I, but are briefly provided here. We selected M giants using NIR color cuts, similar to the Majewski et al. (2003) and Sharma et al. (2010) color cuts, but shifted to reduce contamination from K/M dwarfs and K giants. Our NIR targets were matched to SDSS observations, which were used to

Table 1
Distant Stars in the Milky Way

R.A. (deg)	Decl. (deg)	ℓ (deg)	b (deg)	Distance (kpc)	Type	Reference
115.65748	22.97206	197.11	21.07	122 ± 12[a]	RRL	Drake et al. (2013)
261.4764	3.0072	25.62	20.36	126 ± 32[b]	CN	Mauron (2008)
22.4696	3.2119	141.41	−58.275	133 ± 6	BHB	Deason et al. (2012a)
341.6206	−27.4501	24.98	−62.31	145 ± 36[b]	CN	Mauron et al. (2005)
4.4821	0.0631	105.07	−61.64	151 ± 7	BHB	Deason et al. (2012a)
136.4432	20.4106	207.52	38.35	153 ± 38[b]	CN	Deason et al. (2012a)
195.3269	0.4975	308.42	63.26	161 ± 40[b]	CN	Mauron (2008)
116.07282	25.54249	194.68	22.34	238 ± 64	M giant	This paper
3.89882	1.93044	104.97	−59.69	274 ± 74	M giant	This paper

Notes. We present stars with estimated distances >120 kpc.
[a] Assuming a 10% uncertainty in distance, as explained in Drake et al. (2013).
[b] Following Deason et al. (2012a), we present the mean distance estimated using the Totten et al. (2000) and Mauron et al. (2004) methods, and assume an uncertainty of 25%.

discriminate against quasars. Reddening is small throughout the sample. For example, $E(B-V)$ values for ULAS J0015+01 and ULAS J0744+25 are 0.03 and 0.04, respectively. We astrometrically screened out M dwarfs using the SDSS-USNOB proper motion catalogs (Munn et al. 2004), supplemented by proper motions derived from SDSS-UKIDSS astrometry. After all cuts were applied, 404 M giant candidates remained. Our initial study netted five M giants, and our spectroscopic campaign is ongoing.

During 2014 November 12–14, we obtained spectra of 32 stars using the Red Channel Spectrograph (RCS; Schmidt et al. 1989) at the 6.5 m MMT observatory at Mount Hopkins, Arizona. We used the RCS in single order mode, employing the 1.″0 slit, 1200 lines mm^{-1} grating centered at 8400 Å and LP-530 long-pass filter, resulting in a resolution of $R \sim 5000$. Due to variable and significant cloud coverage during the first night, we observed relatively bright ($V < 10$) stars previously classified as M giants and M dwarfs to aid in spectroscopic classification. These stars, which serve as high signal-to-noise (S/N) spectral standards, are listed in Table 2. Over the remaining 2 nights, we observed 15 M giant candidates, listed in Table 2. Science observations ranged from 180s to 7200s of total exposure time, broken into multiple exposures to aid in cosmic ray rejection. The data were reduced using an IDL software package based on the MASE (Bochanski et al. 2009) reduction pipeline. Each single-order observation was bias-corrected, flat-fielded, wavelength calibrated, and optimally extracted. Wavelength calibrations were obtained using the HeNeAr arc lamp, and corrected to the heliocentric rest frame. Flux calibration was computed by comparing to standards, with at least one standard being observed per night. The typical S/N of our science observations ranged from ∼10 to 50. The spectra of many of the stars obtained during our run are shown in Figure 1.

3. ANALYSIS

3.1. Spectral Type Estimates

Spectral types for our science targets were estimated using two methods. First, each science spectrum was compared to the 17 giant and dwarf spectra. We visually compared each standard-science spectral pair, and computed the χ^2 residuals over the wavelength regime shown in Figure 1. The spectra of ULAS J0015+01 and ULAS J0744+25 agreed more closely with the giant standards, both visually and with respect to χ^2 residuals.

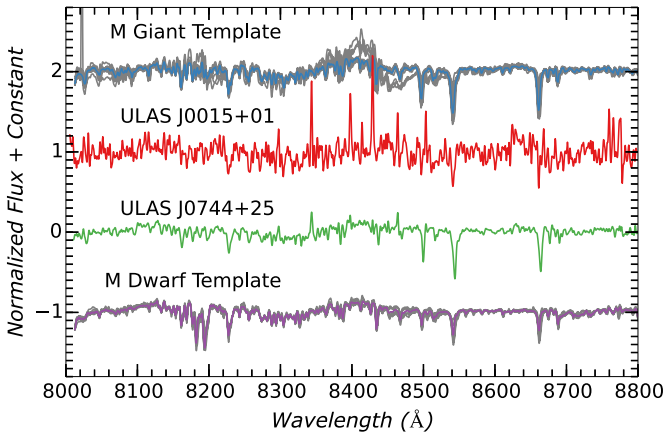

Figure 1. Normalized standard spectra (gray lines) are shown along with the coadded M giant template (blue line) and M dwarf template (purple line). The spectra of ULAS J0015+01 and ULAS J0744+25 are shown in red and green, respectively. Note the strong Na I absorption in the M dwarfs near 8200 Å and the Ca II triplet.

(A color version of this figure is available in the online journal.)

M dwarf and M giant template spectra were also constructed by coadding individual giant and dwarf spectra. Each standard observation (gray lines in Figure 1) was normalized with a fourth-order polynomial to remove the stellar continuum prior to coaddition. The coadded template spectra are shown in Figure 1, along with the spectra of ULAS J0015+01 and ULAS J0744+25. The dominant atomic spectral features in this wavelength regime are the Na I doublet near 8200 Å and the Ca II triplet near 8500 Å. TiO gives rise to the bandheads near 8400 Å, which are easily observed in the M giant spectra, as they change strength drastically throughout the sequence. Telluric features are notable as well. The absorption seen at 8227 Å is due to terrestrial water vapor (Albers 1974). The emission features near 8345, 8400, 8430, 8505, and 8780 Å are due telluric OH emission lines (Cosby et al. 2006).

In Figure 2, we compare the spectra of the distant M giants to the M giant (top) and M dwarf (bottom) templates. The M giant template is a better match to both stars. While the S/N in the ULAS J0015+01 spectrum is only ∼10, the Na I doublet near 8200 Å is not visible. The spectrum of ULAS J0744+25 has a higher S/N (∼20), and is well matched by the M giant template. While M dwarfs exhibit Ca II absorption, the M giant template

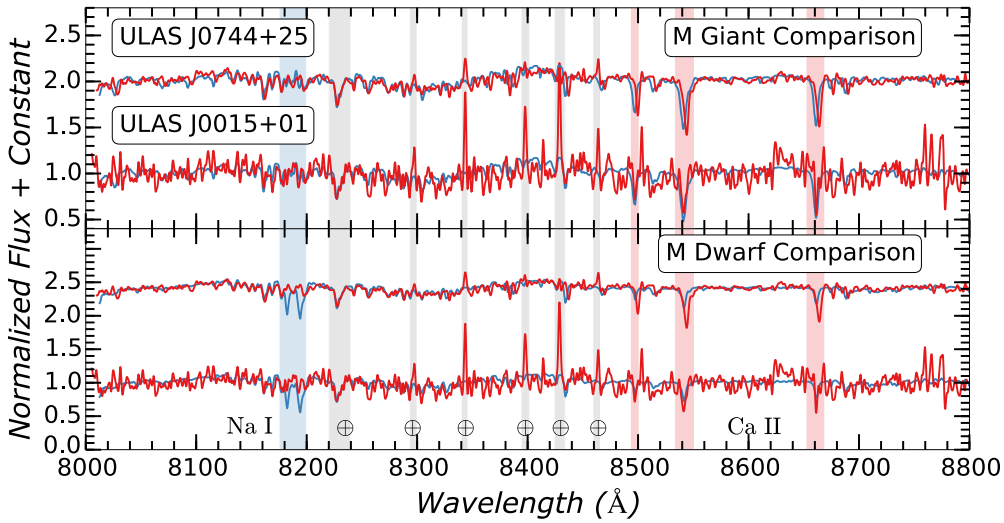

Figure 2. Spectra of ULAS J0744+25 and ULAS J0015+01 (upper and lower red lines, respectively) are compared to the M giant (top panel) and M dwarf templates (bottom panel). The Na I doublet and Ca II triplet are highlighted with blue and red shaded regions. Telluric OH lines are marked with gray shaded regions. The M giant template is a better match to both giants, particularly near Na I.

(A color version of this figure is available in the online journal.)

Table 2
Observed M Giant Candidates and Spectral Standards

Name	R.A. (deg)	Decl. (deg)	J	Sp. Type	RV[a] (km s^{-1})	Notes
ULAS J001535.72+015549.6	3.89882	1.93045	17.73	M giant	-58 ± 10	M giant at ∼274 kpc.
ULAS J021121.56−003808.5	32.83984	−0.63568	15.58	M dwarf		
ULAS J073223.56+263420.0	113.09816	26.57222	16.49	M dwarf		
ULAS J074150.40+263355.5	115.46001	26.56542	13.88	M dwarf		
ULAS J074417.48+253233.0	116.07282	25.54249	17.28	M giant	86 ± 10	M giant at ∼238 kpc.
ULAS J075202.79+204645.0	118.01162	20.77916	13.41	...		Inconclusive spectrum
ULAS J075525.09+235952.2	118.85454	23.99783	14.64	M giant	99 ± 10	M giant at ∼50 kpc.
ULAS J075554.26+273130.9	118.97609	27.52525	15.23	M giant	17 ± 10	M giant at ∼52 kpc (Paper I)
ULAS J205800.46−003445.3	314.50190	−0.57925	17.63	M dwarf		
ULAS J211225.54−005329.4	318.10643	−0.89151	18.17	M dwarf		
ULAS J223815.77+042531.9	339.56569	4.42554	17.31	M dwarf		
ULAS J225509.66+114543.6	343.79025	11.76211	14.12	M giant	-260 ± 10	M giant at ∼35 kpc.
ULAS J225630.15+065544.8	344.12564	6.92911	17.83	M dwarf		
ULAS J231331.68+065303.0	348.38200	6.88417	18.10	M dwarf		
ULAS J235247.04+023151.5	358.19599	2.53098	17.14	M dwarf		
HD 4647	12.30779	57.07502	3.52	M2 III		Standard
WW Psc	14.95703	6.48322	2.65	M2 III		Standard
V360 And	16.01874	38.68854	3.38	M3 III		Standard
HD 236791	23.71879	59.41716	4.97	M3 III		Standard
BD+18 372	43.65878	19.34401	6.12	M3 III		Standard
RZ Ari	43.95208	18.33164	0.22	M6 III		Standard
HD 17993	44.123918	62.60961	3.44	M1 III		Standard
EH Cet	44.26905	4.50102	2.18	M4 III		Standard
SS Cep	57.37506	80.32247	0.76	M5 III		Standard
HD 24410	58.99011	57.67356	3.02	M8 III		Standard
GX And	4.59536	44.02295	5.25	M2 V		Standard
GQ And	4.60624	44.02712	6.79	M6 V		Standard
V596 Cas	29.84798	58.52113	7.79	M4 V		Standard
GJ 3136	32.22332	49.44906	8.42	M5 V		Standard
HD 15285	36.94109	4.43215	5.99	M1 V		Standard
HIP 20745	66.67843	12.68658	7.82	M0 V		Standard
YZ Cmi	116.16739	3.55245	6.58	M5 V		Standard

Note. [a] Radial velocities in the heliocentric rest frame.

is a better match on the blue side of the spectrum, and displays no Na I absorption. Furthermore, if either star was an M dwarf, the Na I doublet would be of similar strength to the water vapor near 8227 Å. However, there are no strong absorption bands in this regime. We note that low-mass subdwarfs also have weakened Na I absorption. Recently, Savcheva et al. (2014) prepared a catalog of 3517 low-mass subdwarfs with SDSS spectra. Less than 1% of these stars would have passed our

Table 3
Distance Estimates of ULAS J0015+01 and ULAS J0744+25

Method	Description	Assumed [Fe/H]	d (kpc)[a]	d (kpc)[b]
Nikolaev & Weinberg (2000)	$M_K = -5.5$	~ -0.7	276 ± 69	224 ± 56
Yanny et al. (2009)	$M_g = -1.0$	~ -0.8	271 ± 68	294 ± 74
Yanny et al. (2009)	$M_r \sim -2.3$	~ -0.8	262 ± 66	264 ± 66
Sharma et al. (2010)	$M_K = 3.26 - 9.42 \times (J-K)$	$\gtrsim -1$	415 ± 104	347 ± 87
Palladino et al. (2012)	$M_i = -1.5$	~ 0	133 ± 33	128 ± 32
Palladino et al. (2012)	$M_z = -3.5$	~ 0	281 ± 70	265 ± 66
Bovy et al. (2012)	$P(M_H \mid J-K)$	0.0	178 ± 45	134 ± 34
Bovy et al. (2012)	$P(M_H \mid J-K)$	-0.5	281 ± 70	214 ± 53
Bovy et al. (2012)	$P(M_H \mid J-K)$	-1.0	354 ± 89	274 ± 68
Comparison to EH Cet	$M_J \sim -4.6$	...	290 ± 73	238 ± 59
Adopted distance	Mean	...	274 ± 74	238 ± 64

Notes.
[a] Distance estimates for ULAS J0015+01.
[b] Distance estimates for ULAS J0744+25.

color and proper motion cuts. We visually inspected the SDSS spectra of subdwarfs that did, and all displayed prominent Na I absorption. Thus, ULAS J0015+01 and ULAS J0744+25 were classified as M giants. The M giant with the closest match to both stars, both visually and with respect to χ^2 was EH Cet, an M4 III giant with an $M_J = -4.6$ (van Leeuwen 2007).

3.2. Distance Estimates

As noted in Paper I, precise photometric distance estimates of M giants are notoriously difficult to produce. Depending on the relation assumed, the absolute magnitude is independent of color (i.e., Nikolaev & Weinberg 2000; Yanny et al. 2009), relates linearly with $J-K$ color (Sharma et al. 2010) or can be estimated using stellar evolution models (Bovy et al. 2012). For each star, we computed distances with six different techniques: either assuming [Fe/H] $= 0.0, -0.5, -1.0$ and employing the Bovy et al. (2012) method, using the absolute magnitude relations from Sharma et al. (2010), Nikolaev & Weinberg (2000), Yanny et al. (2009), and Palladino et al. (2012), or assuming the M_J of EH Cet. The distance estimates are contained in Table 3. For each distance estimate, we assumed an uncertainty of 25%, which is similar to the uncertainty assumed for carbon giants (Mauron et al. 2005; Deason et al. 2012a).

Six of the ten estimates indicate a distance between 260 and 290 kpc for ULAS J0015+01. For ULAS J0744+25, 7 of the 10 distance estimates fall between 210 and 290 kpc. For both stars, the assumed [Fe/H] has a large effect on the distance estimate. For all of the metallicities used in this analysis, the distance to ULAS J0015+01 is $\gtrsim$180 kpc, making it the most distant MW star known to date. Both stars are best matched to the spectrum of EH Cet. The absolute magnitude of EH Cet yields distances of 290 ± 73 and 238 ± 59 for ULAS J0015+01 and ULAS J0744+25, respectively. These values happen to be close to the mean values from all of the distance estimates. Therefore, we adopt the mean distance for each star with the standard deviation of all measurements as the uncertainty and report them in Tables 1 and 3.

3.3. Radial Velocity Measurements

We measured the radial velocity of each M giant by cross-correlating the spectrum against SDSS spectra of M giants. In Paper I, we recovered four M giants in the SDSS database, with typical uncertainties of 10 km s^{-1}. Given the limited wavelength range sampled by MMT, we sought to minimize the effect of exactly which region was selected for cross-correlation. Each science target was correlated against each SDSS M giant spectrum 1000 times, slightly adjusting the starting and end points of the region used for correlation each time. Telluric regions were masked out during the RV measurement. The mean radial velocity and standard deviation was recorded for each SDSS star. The mean heliocentric radial velocity of ULAS J0015+01, measured against all four SDSS M giants, was -57 ± 10 km s^{-1}. The measured velocity of ULAS J0744+25 was 86 ± 10 km s^{-1}. We converted these velocities using the circular speed (240 km s^{-1}) and solar motion used in Deason et al. (2012a), resulting in Galactocentric velocities of 52 ± 10 km s^{-1} for ULAS J0015+01 and 24 ± 10 km s^{-1} for ULAS J0744+25. These velocities are consistent with the relatively cold velocity dispersions seen at large distances (Deason et al. 2012a). We discuss the implication of these velocities on the origins of these stars in the following section.

4. RESULTS AND CONCLUSIONS

The origins of ULAS J0015+01 and ULAS J0744+25 are interesting, given their large distances from the MW. They are at least three times as distant as the Large Magellanic Cloud, and potentially more distant than Leo I and Leo II (Harrington & Wilson 1950). Both stars are near the MW's virial radius, where gas densities are extremely low, and star formation is virtually non-existent. Thus, it would be overwhelmingly unlikely that either star formed in situ.

Given the largely accepted accretion model for the formation of the MW's halo, the most natural hypothesis for the origin of these stars is accretion from a dwarf galaxy (e.g., Bullock & Johnston 2005; Zolotov et al. 2009). Such tidal stripping is well mapped in the inner halo, which is dominated by the Sgr dwarf and its well-mapped tidal tails (Majewski et al. 2003; Belokurov et al. 2014). However, only one stream has been identified at $d > 100$ kpc (Drake et al. 2013). We compared the position and radial velocities of both stars to a model of Sgr (Law & Majewski 2010). Unlike the closer M giants associated with Sgr in Paper I, we did not definitively associate these M giants with Sgr. However, we do note that both stars lie close to the Sgr plane, with ULAS J0744+25 at $(\Lambda, B)_{\rm Sgr} \sim (190.2, 4.7)$, and ULAS J0015+01 at $(\Lambda, B)_{\rm Sgr} \sim (81.8, -16.2)$. Thus, an association with Sgr cannot be ruled out. Furthermore, ULAS

J0015+01 is spatially coincident with the apocenter of the Sgr trailing arm, while ULAS J0744+25 is spatially coincident with the Pisces overdensity (Sharma et al. 2010). Despite being within $\sim 10^{\circ}$ of these structures, both stars have much larger distances.

Despite differences in formation history and halo masses, simulations predict that the majority of stars at $d > 150$ kpc have been accreted less than 9 Gyr ago, suggesting recent accretion is important in the outer halo (Zolotov et al. 2009). Models also predict significantly less substructure with $d \gtrsim 160$ kpc and a stellar density over four orders of magnitude smaller than the solar radius (Bullock & Johnston 2005). While the predicted amount of substructure in the outer halo is small, our experiment was designed to target any trace of this population. Therefore, it is possible that ULAS J0015+01 and ULAS J0744+25 have been stripped from substructure accreted in the last 10 Gyr. With more complete maps and UKIDSS sky coverage, this hypothesis can be more fully explored.

An alternative hypothesis for these stars' origin is ejection from the MW. Both star–binary (i.e., disk ejection) and star–black hole (i.e., hypervelocity) interactions can eject stars (i.e., Zhang et al. 2013; Perets & Šubr 2012). To test this mechanism, we calculated the time it took each star to travel to its current position and velocity, assuming it was formed near the solar circle and was ejected. Since the halo is the dominant potential at these distances, we used a spherical Navarro-Frenk-White halo (Navarro et al. 1996) to model the Galactic potential:

$$\Phi(r) = -\frac{GM_{\rm vir}}{af(c)}\frac{\ln(1+r/a)}{r/a}, \quad (1)$$

where the scale radius a is related to the concentration c of the halo via $a \equiv r_{\rm vir}/c$, and the concentration constant $f(c)$ is

$$f(c) \equiv \ln(1+c) - \frac{c}{1+c}. \quad (2)$$

Recent estimates of the concentration parameter c, range from $\sim$18 to 24 (Battaglia et al. 2005; Deason et al. 2012b; Smith et al. 2007). As mentioned above, the current estimated for the virial mass of the MW range from ~ 0.7 to $2 \times 10^{12}\ M_{\odot}$ (Sofue 2012; Deason et al. 2012b; Burch & Cowsik 2013; Irrgang et al. 2013). Thus, we adopted the middle values of the MW's mass ($1.4 \times 10^{12}\ M_{\odot}$) and concentration parameter ($c = 20$) as fiducial values for the MW potential.

First, we calculated the speeds with which the stars would have left the disk, along with the corresponding apocenters. Assuming each star started near the solar circle (8 kpc), the initial Galactocentric velocities were similar: $v_{\rm r,J0015+01} = 572$ km s^{-1} and $v_{\rm r,J0744+25} = 563$ km s^{-1}. The additional potential terms of the disk and bulge were ignored, but they would serve to increase these speeds. Even without these Galactic components, the necessary speed for each star to reach its current distance is comparable to the measured escape velocity of the MW at the solar circle (500–600 km s^{-1}; Smith et al. 2007). This suggests that the stars were unlikely to be ejected, as the mechanisms that can produce these speeds are relatively rare. Hypervelocity star ejection rates are $\sim 1 \times 10^{-4}$ yr^{-1} (i.e., Zhang et al. 2013), while the rate of 600 km s^{-1} disk runaway ejections is $\sim 1 \times 10^{-6}$ yr^{-1} (i.e., Perets & Šubr 2012).

Next, we calculated the time needed to reach each stars' current position. Using the fiducial model, it would take both stars $\sim$1.5 Gyr to reach their current position, while moving outward. We varied the mass and concentration of the halo to compute a range of travel times, which were the same for both stars and varied from $\sim$1 to 3 Gyr. We will directly test the ejection hypothesis as our sample grows. If ejection is important in placing M giants at these distances, there should be more stars seen in the direction of rotation, since they would gain a $\sim$240 km s^{-1} boost from the MW's rotation.

Another hypothesis for the origin of these stars is their membership in a previously unseen dwarf galaxy. Nearby MW dwarf spheroidals (Draco, Ursa Minor, Sculptor, Carina, Fornax) do not host obvious M giant populations as cataloged by 2MASS with our NIR cuts applied. This paucity of 2MASS M giants in MW dwarfs is not surprising, given 2MASS's faint limit and the low metallicities of the dwarfs. However, Carina (Fe/H $= -1.72$; McConnachie 2012) and Fornax (Fe/H $= -0.99$; McConnachie 2012) each have one to two candidate M giant stars in 2MASS at the correct photometric distances for membership. Assuming that a galaxy capable of hosting an M giant has a mean [Fe/H] $\gtrsim -1.0$, we used the stellar mass-metallicity relation to estimate a $M_V \lesssim -13$ for any unseen dwarf galaxy that could host these stars (Kirby et al. 2013). For such a dwarf to have escaped detection, it would have to be extremely low surface brightness ($\mu_{V,} \gtrsim 30$ mag arcsec^{-2}). Although unseen, the existence of such ghostly objects has been predicted (Bullock et al. 2010; Bovill & Ricotti 2011). To test this hypothesis, we constructed the SDSS $g, g-r$ color–magnitude diagram (CMD) within 15 arcmin of each star. These CMDs were binned and subtracted with a control CMD from a nearby field of the same area. Visual inspection of the subtracted CMDs revealed no obvious detection of any associated red giant branches or Sgr turnoff stars near either M giant. Multi-object spectroscopy of surrounding stars with $r > 20$ mag could provide a test this hypothesis, along with deep search for RR Lyrae stars near each M giant.

After observing 15 M giant candidates, our spectroscopic campaign confirmed four new M giants in the MW's halo. This selection efficiency is in-line with our initial study ($\sim$20%, Paper I) and we expect that $\sim$70 M giants will be recovered from our sample. By identifying more of these stars spectroscopically, we hope to further refine our selection criteria. This will be important for identifying M giants in the next generation of large surveys, such as *Gaia* and LSST (Perryman et al. 2001; Ivezic et al. 2008). While these stars will be too faint for reliable parallax measurements with *Gaia*, they may be able to recover proper motions in the halo. For example, an M giant at *Gaia*'s faint limit ($G = 20$), with a distance of 200 kpc and a tangential velocity of 100 km s^{-1} will have a proper motion of $\sim 100\ \mu$as yr^{-1}. *Gaia*'s expected proper motion uncertainty at $G = 20$ will be $\sim 50\ \mu$as yr^{-1}, resulting in a 2σ measurement (de Bruijne 2012).

J.J.B. and B.W. thank the NSF for support under grants NSF AST-1151462 and PHYS-1066293. A.A.W acknowledges NSF grants AST-1109273, AST-1255568, and the RCSA's Cottrell Scholarship. We thank Jonathan Hargis, Alis Deason, Wyn Evans, Vasily Belokurov and Kathyrn Johnston for helpful conversations.

REFERENCES

Albers, H. 1974, ApJ, 189, 463
Battaglia, G., Helmi, A., Morrison, H., et al. 2005, MNRAS, 364, 433
Bell, E. F., Zucker, D. B., Belokurov, V., et al. 2008, ApJ, 680, 295
Belokurov, V., Koposov, S. E., Evans, N. W., et al. 2014, MNRAS, 437, 116
Bochanski, J. J., Hennawi, J. F., Simcoe, R. A., et al. 2009, PASP, 121, 1409

Bochanski, J. J., Willman, B., West, A. A., Strader, J., & Chomiuk, L. 2014, AJ, 147, 76 (Paper I)
Bovill, M. S., & Ricotti, M. 2011, ApJ, 741, 18
Bovy, J., Allende Prieto, C., Beers, T. C., et al. 2012, ApJ, 759, 131
Brown, W. R., Geller, M. J., Kenyon, S. J., & Kurtz, M. J. 2005, ApJL, 622, L33
Bullock, J. S., & Johnston, K. V. 2005, ApJ, 635, 931
Bullock, J. S., Stewart, K. R., Kaplinghat, M., Tollerud, E. J., & Wolf, J. 2010, ApJ, 717, 1043
Burch, B., & Cowsik, R. 2013, ApJ, 779, 35
Cosby, P. C., Sharpee, B. D., Slanger, T. G., Huestis, D. L., & Hanuschik, R. W. 2006, JGRA, 111, 12307
de Bruijne, J. H. J. 2012, Ap&SS, 341, 31
Deason, A. J., Belokurov, V., Evans, N. W., et al. 2012a, MNRAS, 425, 2840
Deason, A. J., Belokurov, V., Evans, N. W., & An, J. 2012b, MNRAS, 424, L44
Drake, A. J., Catelan, M., Djorgovski, S. G., et al. 2013, ApJ, 765, 154
Harrington, R. G., & Wilson, A. G. 1950, PASP, 62, 118
Helmi, A., Ivezić, Ž., Prada, F., et al. 2003, ApJ, 586, 195
Irrgang, A., Wilcox, B., Tucker, E., & Schiefelbein, L. 2013, A&A, 549, A137
Ivezic, Z., Tyson, J. A., Acosta, E., et al. 2008, arXiv:0805.2366
Kirby, E. N., Cohen, J. G., Guhathakurta, P., et al. 2013, ApJ, 779, 102
Klypin, A., Zhao, H., & Somerville, R. S. 2002, ApJ, 573, 597
Law, D. R., & Majewski, S. R. 2010, ApJ, 714, 229
Lawrence, A., Warren, S. J., Almaini, O., et al. 2007, MNRAS, 379, 1599
Majewski, S. R., Skrutskie, M. F., Weinberg, M. D., & Ostheimer, J. C. 2003, ApJ, 599, 1082
Mauron, N. 2008, A&A, 482, 151
Mauron, N., Azzopardi, M., Gigoyan, K., & Kendall, T. R. 2004, A&A, 418, 77
Mauron, N., Kendall, T. R., & Gigoyan, K. 2005, A&A, 438, 867
McConnachie, A. W. 2012, AJ, 144, 4
Munn, J. A., Monet, D. G., Levine, S. E., et al. 2004, AJ, 127, 3034
Navarro, J. F., Frenk, C. S., & White, S. D. M. 1996, ApJ, 462, 563
Nikolaev, S., & Weinberg, M. D. 2000, ApJ, 542, 804
Palladino, L. E., Holley-Bockelmann, K., Morrison, H., et al. 2012, AJ, 143, 128
Perets, H. B., & Šubr, L. 2012, ApJ, 751, 133
Perryman, M. A. C., de Boer, K. S., Gilmore, G., et al. 2001, A&A, 369, 339
Piffl, T., Scannapieco, C., Binney, J., et al. 2014, A&A, 562, A91
Savcheva, A., West, A. A., & Bochanski, J. J. 2014, AJ, submitted
Schlaufman, K. C., Rockosi, C. M., Allende Prieto, C., et al. 2009, ApJ, 703, 2177
Schmidt, G. D., Weymann, R. J., & Foltz, C. B. 1989, PASP, 101, 713
Sharma, S., Johnston, K. V., Majewski, S. R., et al. 2010, ApJ, 722, 750
Skrutskie, M. F., Cutri, R. M., Stiening, R., et al. 2006, AJ, 131, 1163
Smith, M. C., Ruchti, G. R., Helmi, A., et al. 2007, MNRAS, 379, 755
Sofue, Y. 2012, PASJ, 64, 75
Totten, E. J., Irwin, M. J., & Whitelock, P. A. 2000, MNRAS, 314, 630
van Leeuwen, F. 2007, A&A, 474, 653
Xue, X.-X., Ma, Z., Rix, H.-W., et al. 2014, ApJ, 784, 170
Yanny, B., Newberg, H. J., Johnson, J. A., et al. 2009, ApJ, 700, 1282
York, D. G., Adelman, J., Anderson, J. E., Jr., et al. 2000, AJ, 120, 1579
Zhang, F., Lu, Y., & Yu, Q. 2013, ApJ, 768, 153
Zolotov, A., Willman, B., Brooks, A. M., et al. 2009, ApJ, 702, 1058